Traveling Wave Ultrasonic Motor: Free Stator Modeling

Mojallali, H.; Amini, R.; Izadi-Zamanabadi, Roozbeh; Helbo, Jan

Publication date:
2004

Document Version
Også kaldet Forlagets PDF

Traveling Wave Ultrasonic Motor: Free Stator Modeling

H. Mojallali, R. Amini,
R. Izadi-Zamanabadi, J. Helbo

ISBN: 87-90661-21-3

Department of Control Engineering
Aalborg University
Fredrik Bajers Vej 7, DK-9220 Aalborg Ø, Denmark.

Preface

In this report, an equivalent circuit model for the free stator of piezoelectric motor is presented while the circuit elements have complex values. The mechanical, dielectric and piezoelectric losses associated with the vibrator are accounted for by the imaginary components of the circuit elements. It is shown that the calculation of the circuit parameters from the complex elastic, dielectric and piezoelectric material constants is straightforward and the model accuracy is verified with experiments.

Contents

List of Figures

List of Tables

Nomenclature

Physicsal Parameters

There are a number of physical parameters for which symbols are used.

S_1	Mechanical strain vector in 1-direction
T_1	Mechanical stress vector in 1-direction caused by a pressure in 1-direction
E_3	Electrical field vector in 3-direction
D_3	Electrical displacement vector in 3-direction
s_{11}^E	Element $(1,1)$ in elastic compliance matrix of piezoelectric material at constant electrical field
d_{31}	Element $(3,1)$ in piezoelectric constant matrix
ϵ_{33}^T	Element $(3,3)$ of electrical permitivity matrix at constant stress
k_{31}	Electromechanical coupling constant
ρ	Mass density of the piezoelectric material
F_1, F_2	External forces acting on the pirzoelectric bar laterally
l	Length of the piezo bar
h	Height of the piezo bar
W	Width of the piezo bar
ζ	Displacement of the vibrating edge of piezoelectric bar
v_b^E	Velocity of longitudinal waves in the piezoelectric bar
ω	Angular frequency of electrical field
E_0	Amplitude of electrical field
U_1, U_2	Velocities of piezoelectric bar at each end
$I(t)$	Electric current flowing into the piezo ceramic
C_d	Clamped capacitance of the piezoelectric
N	Electromechanical transformed (force factor)
Y_m	Transformed motional admittance
Y_d	Damping admittance
y_m	Motional admittance
f_s	Resonance frequency of the piezoelectric ring
f_p	Anti-resonance frequency of the piezoelectric ring
R_d	A resistor representing the electromechanical losses
$Y(\omega)$	Admittance of the unloaded stator at angular frequency ω
$Z(\omega)$	Impedance of the unloaded stator at angular frequency ω
B	Susceptance of unloaded stator
G	Conductance of unloaded stator
X	Reactance of unloaded stator
R	Resistance of unloaded stator

1 Introduction

The traveling wave piezoelectric motor has excellent performance and many useful features such as high holding torque, high torque at low speed, quiet operation (ultrasonic), simple structure, compactness in size and no electromagnetic interferences [2]. However, the mathematical model of the piezoelectric motor is complex and difficult to drive due to its driving principle based on high-frequency mechanical vibrations and frictional force. With the help of the model, the influence of diverse factors like material and construction parameters, electrical excitation, load torque and axial applied force can be examined. Also, achieving a good model is very important for studying and design of control systems for the motor. Despite many reported attempts, the modeling of this device is still a challenging problem. It is frequently more convenient to use the equivalent circuit approach for modeling where both the electrical and mechanical portions of piezoelectric motor are represented by electrical equivalents [2]. The equivalent circuit can be derived using the equation of motion and appropriate piezoelectric equations. Equivalent circuit modeling of traveling wave ultrasonic motor has been the subject of extensive research all over the world and important contributions have been established in [2]. In [3, 4] a systematic modeling approach has been reported for Shinsei type USR60 as a case study, but the authors have used simplification assumption for modeling and the presented models fit only for fundamental resonance frequency. In this report, an equivalent circuit model for the free stator of rotary piezoelectric motor proposed that the circuit elements are complex. Also, the proposed approach can be applied for all rotary type of piezoelectric motor. By comparing with the measurements data, it is shown that the proposed model describes the behavior of the motor around the fundamental frequency substantially more precise than the former models.

In this report, first, the background of the equivalent circuit modeling method is described. Then, complex numerical approach for equivalent circuit modeling is introduced and the measuring methods for complex material constants are presented. Finally, the validation of model is accomplished by comparing the simulation results with the experimental measurements.

2 Modeling

2.1 Equivalent circuit modeling of a free stator

We can consider the stator ring as a straight beam with infinite length as shown in Fig. 1. Assume a bar of piezoelectric material lied along the x-direction, with

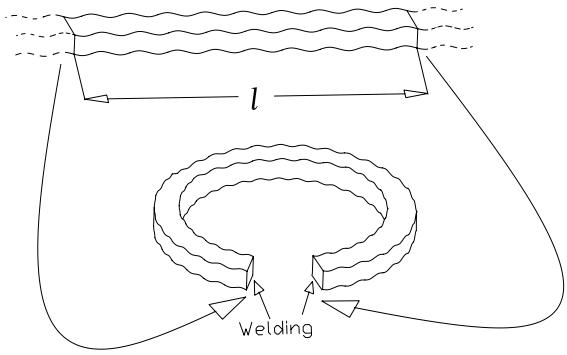

Figure 1: The stator of traveling wave motor regarded as a straight beam

electrode faces normal to the z-direction as shown in Fig. 2, and with both cross-sectional dimensions small compared to its length. With this assumption, a bending deformation of a transverse type (T-effect) driven by an alternative voltage is generated along the straight beam. The fundamental (T, E)-type relation is [5]

$$S_1 = s_{11}^E T_1 + d_{31} E_3 \tag{1}$$

$$D_3 = d_{31} T_1 + \epsilon_{33}^T E_3 \tag{2}$$

and the wave equation which is derived using Newton's equation for an element of

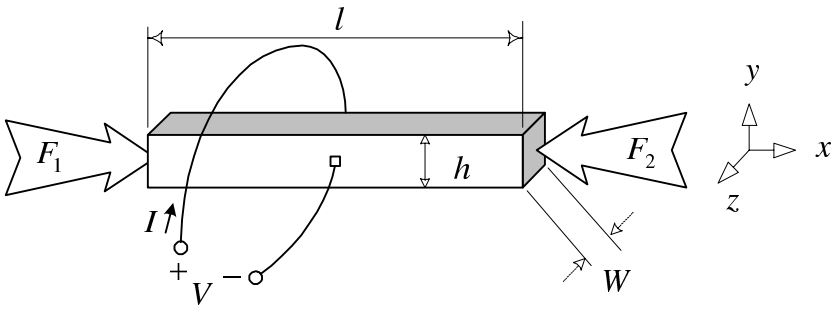

Figure 2: One dimensional actuator using T-effect under z-direction poling

volume $(dxdydz)$ is

$$\rho \frac{\partial^2 \zeta_1}{\partial t^2} dxdydz = \frac{\partial T_1}{\partial x} dxdydz \tag{3}$$

where ζ_1 is the displacement of the vibrating edge and ρ is the mass density of the beam. Substituting from Eq. (1) and recalling that $S_1 = \frac{\partial \zeta_1}{\partial x}$, yield

$$\rho \frac{\partial^2 \zeta_1}{\partial t^2} = \frac{1}{s_{11}^E} \frac{\partial^2 \zeta_1}{\partial t^2} - \frac{d_{31}}{s_{11}^E} \frac{\partial E_3}{\partial x} \tag{4}$$

As it is shown in Fig. 2, two opposite surfaces of the rectangular cube are coated by electrodes and connected to the power supply. Each of the coated surfaces is equipotential and the width of the bar, W, is very small in comparison with its length, l. Therefore E_3 is independent of x and $\frac{\partial E_3}{\partial x} = 0$.

$$\frac{\partial^2 \zeta_1}{\partial t^2} = \frac{1}{\rho s_{11}^E} \frac{\partial^2 \zeta_1}{\partial x^2} = (v_b^E)^2 \frac{\partial^2 \zeta_1}{\partial x^2} \tag{5}$$

and

$$v_b^E = \frac{1}{\sqrt{\rho s_{11}^E}} \tag{6}$$

where v_b^E is the velocity of longitudinal waves in the piezoelectric bar [6]. The solution of (5) gives the formula which describes the transverse vibration in the beam

$$\zeta_1 = \left[A sin(\frac{\omega x}{v_b^E}) + B cos(\frac{\omega x}{v_b^E}) \right] e^{j\omega t} \tag{7}$$

Now, we consider the block equivalent circuit shown in Fig. 3 for length expander bar with electric field perpendicular to the length direction. For a sinusoidal

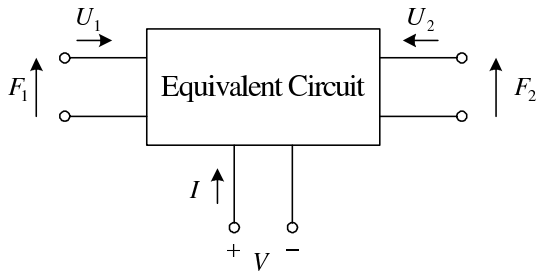

Figure 3: Block equivalent circuit for length expander bar with electric field perpendicular to the length

excitation $E_3 = E_0 e^{j\omega t} = \frac{V(t)}{W}$, the constants A and B in Eq. (7) are evaluated in terms of the velocities U_1 and U_2

$$\dot{\zeta}_1|_{x=0} = +U_1 \qquad , \qquad \dot{\zeta}_1|_{x=l} = -U_2 \tag{8}$$

$$\begin{cases} A = -\frac{1}{j\omega} \left(\frac{U_2}{sin \frac{\omega l}{v_b^E}} + \frac{U_1}{tan \frac{\omega l}{v_b^E}} \right) e^{-j\omega t} \\ B = \frac{1}{j\omega} U_1 e^{-j\omega t} \end{cases} \tag{9}$$

The forces at the both faces can be expressed using Eqs. (1), (2), (7) and (9). At $x = 0$, $F_1 = -hWT_1|_{x=0}$ gives

$$F_1 = -\frac{hW}{s_{11}^E} A \frac{\omega}{v_b^E} e^{j\omega t} + \frac{hd_{31}}{s_{11}^E} V \tag{10}$$

Also, at $x = l$, $F_2 = -hWT_1|_{x=l}$ gives

$$F_2 = -\frac{hW}{s_{11}^E}\big(A\frac{\omega}{v_b^E}cos\frac{\omega l}{v_b^E} - B\frac{\omega}{v_b^E}sin\frac{\omega l}{v_b^E}\big)e^{j\omega t} + \frac{hd_{31}}{s_{11}^E}V \tag{11}$$

By substituting Eq. (9) in the above equations and after rearranging the terms, Eqs. (10) and (11) become

$$F_1 = \frac{hW}{js_{11}^E v_b^E sin\frac{\omega l}{v_b^E}}U_2 + \frac{hW}{js_{11}^E v_b^E tan\frac{\omega l}{v_b^E}}U_1 + \frac{hd_{31}}{s_{11}^E}V \tag{12}$$

$$F_2 = \frac{hW}{js_{11}^E v_b^E tan\frac{\omega l}{v_b^E}}U_2 + \frac{hW}{js_{11}^E v_b^E sin\frac{\omega l}{v_b^E}}U_1 + \frac{hd_{31}}{s_{11}^E}V \tag{13}$$

Eqs. (12) and (13) can be written in the following form

$$\begin{aligned} F_1 &= Z_1U_2 + (Z_1 + Z_2)U_1 + NV \\ F_2 &= (Z_1 + Z_2)U_2 + Z_1U_1 + NV \end{aligned} \tag{14}$$

where

$$\begin{cases} Z_1 = \frac{hW}{js_{11}^E v_b^E sin\frac{\omega l}{v_b^E}} \\ Z_2 = \frac{jhW}{s_{11}^E v_b^E}tan\frac{\omega l}{2v_b^E} \end{cases} \tag{15}$$

The electric current flowing into the piezo ceramic can be evaluated as follows

$$I(t) = \int_0^h \int_0^l j\omega D_3 dxdy \tag{16}$$

By using $E_3 = \frac{V(t)}{W}$ and after inserting Eq. (1) into (2), the following relation is obtained

$$D_3 = \frac{d_{31}}{s_{11}^E}S_1 + \epsilon_{33}^S\frac{V(t)}{W} \tag{17}$$

where

$$\begin{cases} \epsilon_{33}^S = \epsilon_{33}^T(1 - k_{31}^2) \\ k_{31}^2 = \frac{d_{31}^2}{s_{11}^E\epsilon_{33}^T} \end{cases} \tag{18}$$

and k_{31} is the electromechanical coupling factor. By using Eqs. (16) and (17), the electric current is expected as

$$I = -\frac{hd_{31}}{s_{11}^E}U_1 - \frac{hd_{31}}{s_{11}^E}U_2 + j\omega\frac{\epsilon_{33}^S hl}{W}V(t) \tag{19}$$

which can be rewritten as

$$I = -N(U_1 + U_2) + j\omega C_d V(t) \tag{20}$$

where

$$N = \frac{hd_{31}}{s_{11}^E} \qquad , \qquad C_d = \frac{\epsilon_{33}^S hl}{W} \tag{21}$$

and C_d is the clamped capacitance of the piezoelectric from the derived Eqs. (14), (19). The electromechanical equations in the beam are represented by

$$\begin{cases} F_1 = Z_1 U_2 + (Z_1 + Z_2) U_1 + NV(t) \\ F_2 = (Z_1 + Z_2) U_2 + Z_1 U_1 + NV(t) \\ I(t) = -N(U_1 + U_2) + j\omega C_d V(t) \end{cases} \tag{22}$$

Furthermore, the above equations can be shown in the form of six-terminal circuit as shown in Fig. 4 [6]. In the case of the piezoelectric ring, $F_1 = F_2 = F$ and

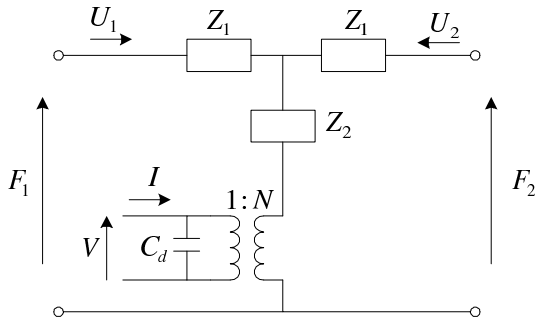

Figure 4: Six-terminal equivalent circuits for length expander bar

the six-terminal equivalent circuit is reduced to four-terminal circuit. Therefore Eq. (22) becomes

$$\begin{cases} F = Z_1 U_2 + (Z_1 + Z_2) U_1 + NV(t) \\ F = (Z_1 + Z_2) U_2 + Z_2 U_1 + NV(t) \\ I(t) = -N(U_1 + U_2) + j\omega C_d V(t) \end{cases} \tag{23}$$

which gives

$$I = -\frac{2N}{2Z_1 + Z_2} F + \big(\frac{2N^2}{2Z_1 + Z_2} + j\omega C_d\big) V \tag{24}$$

Consequently, the admittance Y of the stator is obtained from Eq. (24)

$$Y = \frac{I}{V} = j\omega C_d + \frac{2N^2}{2Z_1 + Z_2} = Y_d + Y_m \tag{25}$$

where Y_d is the damping admittance and Y_m is the transformed motional admittance to the electrical side defined as

$$\begin{aligned} Y_d &= j\omega C_d \\ Y_m &= \frac{2N^2}{2Z_1 + Z_2} = N^2 y_m \end{aligned} \tag{26}$$

here, N is the electromechanical transformer known as the force factor and y_m is the motional admittance

$$y_m = \frac{2}{2Z_1 + Z_2} \tag{27}$$

By using Eqs. (15) and (27), y_m can be rewritten as

$$Y_m = j\omega C_d \frac{k_{31}^2}{1-k_{31}^2} \frac{tan\frac{\omega l}{2v_b^E}}{\frac{\omega l}{2v_b^E}} \tag{28}$$

2.2 Real Numerical Approach

The obtained equation for admittance is not suitable for representation in the form of equivalent circuit because of the involved nonlinear tangent term. The common solution for this issue is to confine the attention to mechanical resonance and antiresonance i.e. to values of ω where $tan\frac{\omega l}{v_b^E} = \infty$ or 0. The tangent function maybe expanded near a resonance by the Mittage-Leffler theorem [7] which is given by

$$\frac{tan(x)}{x} = \sum_{n=1}^{\infty} \frac{P_n}{1-\left(\frac{x}{x_n}\right)^2} \quad , \quad n = 2k \pm 1 \quad k = 1, 2, ... \tag{29}$$

where

$$P_n = \frac{8}{\pi^2 n^2} \quad , \quad x_n = \frac{n\pi}{2} \tag{30}$$

at resonance. By substituting Eq. (29) in Eq. (28), the motional admittance becomes

$$Y_m = \sum_{n=1}^{\infty} j\omega \frac{N^2}{\frac{1}{C_n} - \ell\omega^2} = N^2 y_m \quad , \quad n = 2k \pm 1 \quad k = 1, 2, ... \tag{31}$$

where

$$\begin{cases} \ell = \frac{1}{\omega_n^2 C_n} \\ C_n = \frac{P_n}{N^2} \frac{k_{31}^2}{1-k_{31}^2} C_d \end{cases} \tag{32}$$

Therefore, the electromechanical motional branch of the admittance is expressed by an infinite number of (ℓ, C_n)-series circuits in parallel. Figure 5 demonstrates the circuit. Practically, the fundamental frequency is interesting and useful thus it

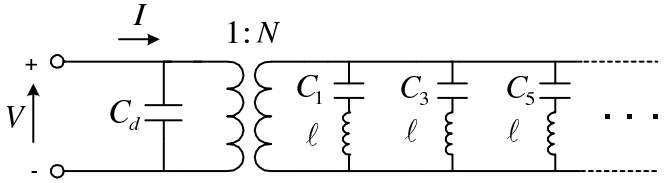

Figure 5: Equivalent circuit model for one phase of the stator over a large span of frequencies

is mandatory to identify the admittance around this frequency and represent the motional admittance with one set of (ℓ, C_1) as it is shown in Figure 6. In order to consider the sources of loss of energy in real stator, the losses of energy within the system at the input terminal and the output terminal should be integrated. This is done by adding a resistor R_d, representing the dielectrical losses, in parallel with the blocking capacitance and another resistance R_1, as the electromechanical losses in series with the motional (ℓ, C_1)-series (Fig. 7). The electromechanical transformer is normally eliminated by transforming the mechanical elements ℓ and C_1 to the

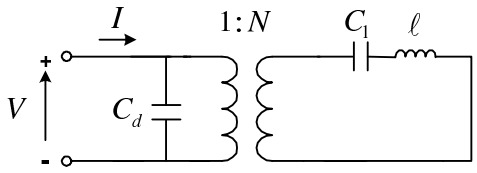

Figure 6: Equivalent circuit model for one phase of stator without losses around the fundamental resonance frequency

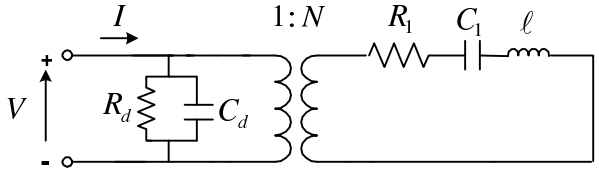

Figure 7: The equivalent circuit model for one phase of the stator integrating the losses around the fundamental resonance frequency

electrical side. The equivalent electrical values of the transported electromechanical elements are

$$R = \frac{R_1}{N^2} \quad , \quad L = \frac{\ell}{N^2} \quad , \quad C = N^2 C_1 \tag{33}$$

and the electrical equivalent circuit model is shown in Fig. 8.

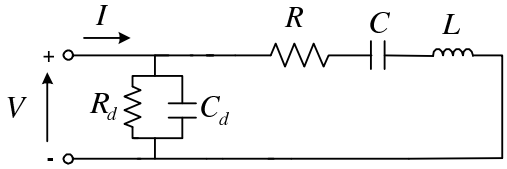

Figure 8: The equivalent circuit modeling for one phase of stator integrating the losses around the fundamental frequency (the mechanical parameters are shown as their electrical equivalents)

2.3 Complex Numerical Approach

As discussed in the previous section, the equation for the admittance of an unloaded stator is described as a function of the frequency ω by the following equation

$$Y = j\omega C_d + j\omega C_d \frac{k_{31}^2}{1 - k_{31}^2} \frac{tan\frac{\omega l}{2v_b^E}}{\frac{\omega l}{2v_b^E}} \tag{34}$$

Substituting Equation (21) into (34) yields

$$Y = j\omega \frac{\epsilon_{33}^T hl}{W} \left(1 - k_{31}^2 + k_{31}^2 \frac{tan\frac{\omega}{4f_s}}{\frac{\omega}{4f_s}}\right) \tag{35}$$

where

$$f_s = \frac{v_b^E}{2l} = \sqrt{\frac{1}{4l^2 \rho s_{11}^E}} \quad , \quad k_{31}^2 = \frac{d_{31}^2}{\epsilon_{33}^T s_{11}^E} \tag{36}$$

The material constants ϵ_{33}^T, s_{11}^E and d_{31} were originally assumed to be real in the derivation of the equations. Holland [8] found that the material constants of piezoelectric materials can be represented by complex numbers with the imaginary parts representing the losses or out-of-phase components.

The admittance Eq. (35) does not change if the material constants are defined as complex numbers. Also, the above equations show that, when ϵ_{33}^T, s_{11}^E and d_{31} are complex, f_s and k_{31} must be also complex. The real and imaginary parts of f_s represent the resonance frequency and the bandwidth of resonance, respectively [9, 10].

The model presented at the previous section uses four real circuit parameters to represent admittance of a unloaded stator. However, Eq. (35) shows that six material constants (the real and imaginary components of ϵ_{33}^T, s_{11}^E, d_{31} or k_{31} are needed to describe the resonance completely when losses are significant. As pointed out in [11], representing the losses of a capacitor or inductor by adding a frequency-independent resistor in parallel with them is less general than is representing these losses by the use of complex circuit components i.e. the obtained resistor becomes frequency dependant.

Therefore, we propose a circuit model which contains three circuit elements, C_0, C and L. The circuit has six parameters and some features that make it an appropriate model for representing the circuit characteristics of an unloaded stator (Fig. 9).

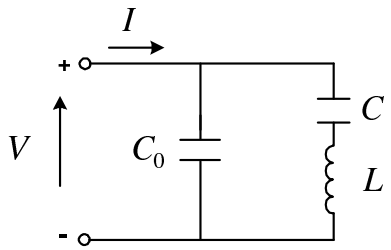

Figure 9: The proposed complex circuit model. The values of all the circuit constants are complex

2.3.1 Measuring Method for Complex Material Constants

The IEEE standard on piezoelectricity [12] describes the resonance-antiresonance (R-A) method for determining the real, but not complex, material constants of piezoelectric. The effect of losses and all the phase information neglected in the IEEE standard method. Also, there are several methods which can be classified as iterative [13–16, 16–19] and non-iterative [9, 10]. The iterative methods use the frequency spectrum of the electrical measurements, within the range of the resonance-antiresonance of the fundamental mode only, to determine all material constants, while the non-iterative methods require some more measurements, away from fundamental resonance, to determine the dielectric constants at constant stress or strain. Also, Du et al. [20–22] introduced an analytical approach to determine complex constants of piezoelectric material. All reported methods normally give accurate results in research work.

In this report, we propose an non-iterative approach similar to Sherrit's, but It's different in the last stage. In other words, we choose a frequency data point in the last stage to fit our model to experimental data. This is the main difference between our approach and Sherrit's. We define the parallel and series resonance frequencies f_s and f_p, as the frequencies which correspond to maxima in the real parts of $\omega Z(\omega)$ and $\frac{Y(\omega)}{\omega}$ respectively. Our definitions are mathematically more correct since f_s, for example, is the frequency at which the expression in parentheses in Eq. (35) has a maximum in its real part. Also, we define frequencies, with complex arguments, which combine the critical frequencies from both the real and imaginary parts of the impedance and admittance spectra. Thus, the series and the parallel resonance frequencies are respectively defined by [1]

$$f_p = f_p^{(1)}\big(1 - j\frac{f_{-\frac{1}{2}}^{(1)p} - f_{+\frac{1}{2}}^{(1)p}}{f_p^{(1)}}\big)^{-\frac{1}{2}} \tag{37}$$

$$f_s = f_s^{(1)}\big(1 - j\frac{f_{-\frac{1}{2}}^{(1)} - f_{+\frac{1}{2}}^{(1)}}{f_s^{(1)}}\big)^{-\frac{1}{2}} \tag{38}$$

$$\tag{39}$$

where all the particular frequencies are shown in Fig. 10. The compliance s_{11}^E is

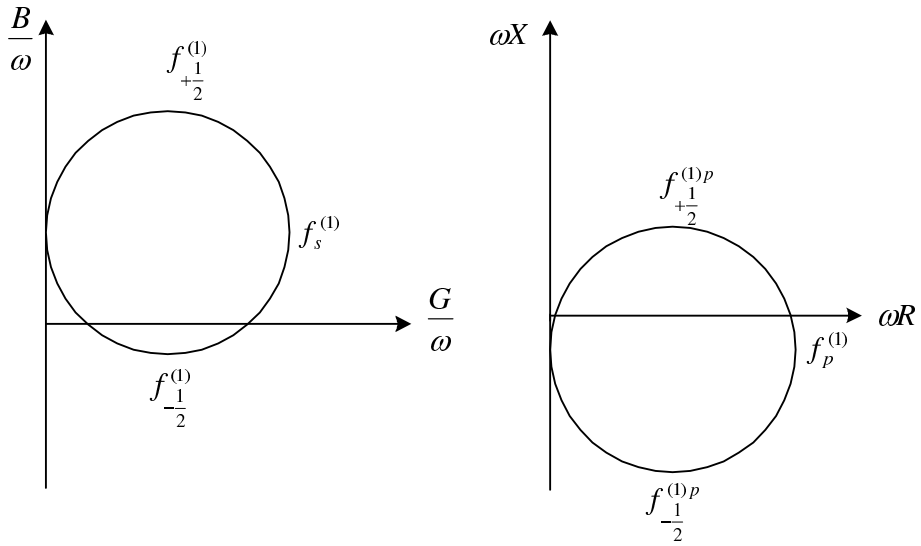

Figure 10: The critical frequencies determined from the modified admittance and impedances locus diagrams which are plots of $\frac{B(\omega)}{\omega}$ versus $\frac{G(\omega)}{\omega}$ and of $\omega X(\omega)$ versus $\omega R(\omega)$. [1]

determined by assuming that the frequency f_s corresponds to the argument of the tangent function equal to $\frac{\pi}{2}$.

$$s_{11}^E = \frac{1}{4\rho l^2 (f_s)^2} \tag{40}$$

The last equation is valid when the magnitudes of the imaginary parts of coefficients are much less than those of their real parts (for example, less than 10 times) [20] .

The complex value of the electromechanical coupling constant, k_{31} , can be evaluated from IEEE standard method [12].

$$k_{31}^2 = \frac{\frac{\pi}{2}\frac{f_p}{f_s} tan(\frac{\pi}{2}\frac{(f_p - f_s)}{f_s})}{1 + \frac{\pi}{2}\frac{f_p}{f_s} tan(\frac{\pi}{2}\frac{(f_p - f_s)}{f_s})} \tag{41}$$

In Eq. (41) , we assume that the frequency f_p is close to the zero point of the admittance. The accuracy of this assumption is dependent on the mechanical quality factor (the real part of s_{11}^E over its imaginary part) [16]. For ideal, no-loss materials, the tangent function in Eq. (35) has a real argument and sweeps from $-\infty$ to $+\infty$ in the vicinity of $\frac{\pi}{2}$. In this case, the zero point of Eq. (35) can be found. However, the zero point usually does not exist for lossy materials. Even for a material with a high mechanical coupling factor, the tangent function in (35) varies in limited range. The error of k_{31}^2 decreases as k_{31}^2 or the mechanical quality factor increases [16]. By using the value of k_{31}^2 and solving Eq. (34) for an arbitrary frequency, f, ϵ_{33}^T will be determined by

$$\epsilon_{33}^T = \frac{Y(\omega)W}{ihl\omega\big(1 - k_{31}^2 + k_{31}^2 \frac{tan(\frac{\omega}{4f_s})}{\frac{\omega}{4f_s}}\big)} \tag{42}$$

Subsequently, the following known equation gives the value of d_{31}^2

$$d_{31}^2 = \epsilon_{33}^T s_{11}^E k_{31}^2$$

The selection of the frequency for solving Eq. (42) should be performed carefully because the variation of the admittance curve around and close to the critical frequencies is very high which brings inaccuracy in calculating the value of ϵ_{33}^T therefore we suggest using a frequency far enough from f_p and f_s e.g. $f = 1.1f_s$ or $f = 0.9f_s$. On the other hand, this selection constitutes an essential rule in fitting the calculated model to the real curve of admittance. If fitting in higher frequencies is desired, f should be chosen bigger than f_p and f_s and contrariwise for lower frequencies. Thus, a hybrid model to get the best result could be accomplished.

2.3.2 The calculation of the circuit parameters from the material constants

This section describes how the complex circuit parameters, C_0, C and L, can be determined from the complex material constants. As the frequency ω tends to zero, the admittance of the unloaded stator shown in Eq. (35) tends to the following value

$$\lim_{\omega \to 0} Y(\omega) = j\omega\epsilon_{33}^T \frac{hl}{W} \tag{43}$$

whereas the impedance of the circuit model in Fig. 9 is

$$\lim_{\omega \to 0} Y(\omega) = j\omega(C_0 + C) \tag{44}$$

A comparison of the two values of Y shows that

$$C_0 + C = \frac{\epsilon_{33}^T hl}{W} \tag{45}$$

The parallel and series resonance of the circuit shown in Fig 8 are

$$f_p = \frac{1}{2\pi\sqrt{L\frac{C_0 C}{C_0+C}}}$$
$$f_s = \frac{1}{2\pi\sqrt{LC}} \tag{46}$$

Finally, the complex circuit constants C_0, L and C may be written in terms of the complex constants k_{31}, s_{11}^E, ϵ_{33}^T, f_p and f_s. Thus

$$C = \frac{f_p^2 - f_s^2}{f_p^2}\frac{\epsilon_{33}^T hl}{W} \tag{47}$$

$$L = \frac{1}{4\pi^2 f_s^2 C} \tag{48}$$

$$C_0 = \frac{\epsilon_{33}^T hl}{W} - C \tag{49}$$

3 Simulation

In this section, the proposed model for unloaded stator modeling is examined on a Shinsei USR60 piezoelectric motor. In [4] Gain-Bandwidth method [23] is used for measuring the real values of the elements of the equivalent circuit. The Gain-Bandwidth method is based on the approximation of Eq. (35) by the first term of Mittage-Leffler expansion introduced in section 2.2. The least approximation error for this expansion occurs at the resonance frequency, f_s. The error of this approximation increases as the difference of f_s and the frequency at which the approximation is performed grows. In addition, this approach neglects the dielectric losses and does not use the phase of the admittance to improve the accuracy. Du et al. in [21] studied the error arising by applying this method.

As the first stage of the simulation, the values of the crucial frequencies (f_s and f_p) are calculated from the curve of the admittance. f_p and f_s are calculated from figures 11a and 11b according to the method described in Section 2.3.1 by Eqs. (37) and (39).

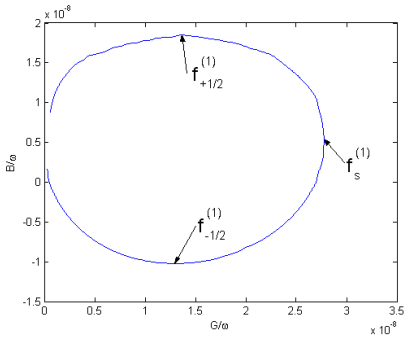

(a) Plot of $\frac{B}{\omega}$ versus $\frac{G}{\omega}$ for identifying the series resonance frequency f_s

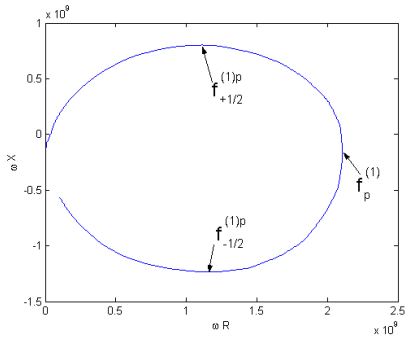

(b) Plot of ωX versus ωR for identifying the parallel resonance frequency f_p

Figure 11: Evaluating the resonance and anti-resonance frequencies by Land's method [1]

Table 1: Values of piezoelectric constants

Material Constant	Value	Unit
Mass Density of the Piezoplate	$\rho = 7650$	$[kg.m^{-3}]$
Length of piezo-plate bar	$l = 2\pi \cdot 26.75 \times 10^{-3}$	$[m]$
Compliance at constant electrical field	$s_{11}^E = 7.7669 \times 10^{-13} - 4.8305 \times 10^{-15} j$	$[m^2.N^{-1}]$
Resonance Frequency	$f_s = 38593 + 120j$	$[Hz]$
Anti-resonance Frequency	$f_p = 39042 + 100j$	$[Hz]$
Intrinsic Coupling Factor	$k_{31}^2 = 0.0282 - 0.0013j$	-

By using Eq. (41), the overall intrinsic coupling factor of the piezomaterial, k_{31}^2 is calculated. Table 1 shows the values of f_s, f_p, s_{11}^E and k_{31}^2.

Two scenarios are evaluated here for simulation and verification of the proposed method. In the first scenario, frequencies higher than the resonance frequency are considered and Eq. (42) is solved for $f = 41000[Hz]$. After calculating the complex values of ϵ_{33}^T and d_{31}, the elements of the equivalent circuit are calculated as shown in table 2. Comparing the magnitude of the admittance of the equivalent circuit and

Table 2: Values of piezoelectric constants in the first scenario

Material Constant	Value	Unit
Di-electric Constant	$d_{31} = 2.0712 \times 10^{-11} - 9.1400 \times 10^{-13} j$	$[C.N^{-1}]$
Electrical Permitivity at Constant Stress	$\epsilon_{33}^T = 1.9566 \times 10^{-8} - 6.8864 \times 10^{-10} j$	$[F.m^{-1}]$
C	$1.6274 \times 10^{-10} - 1.3369 \times 10^{-11} j$	$[F]$
C_0	$6.9625 \times 10^{-9} - 2.3741 \times 10^{-10} j$	$[F]$
L	$0.1039 + 0.0079 j$	$[L]$

the measured admittance of the unloaded stator in frequencies higher than f_s shows that the equivalent circuit models the unloaded stator precisely (See Fig. 12). Also in Fig 12, the admittance curve of our method is compared with another method, based on evaluation of real values for constants and equivalent circuit elements proposed by ElGhouti in [4].

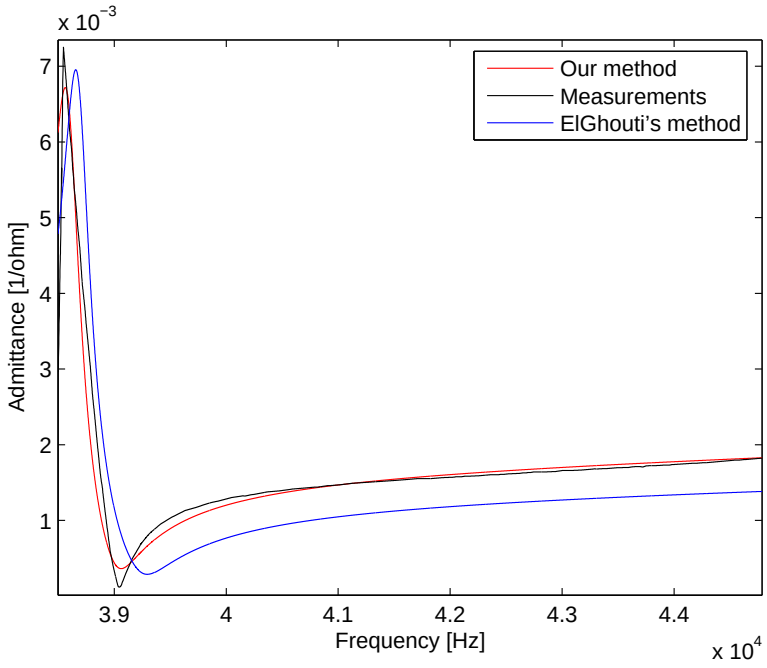

Figure 12: Comparison of the measurement of the admittance with the results of simulation for frequencies higher than resonance frequency, f_s.

In the second scenario, the Eq. (42) is solved for an arbitrary frequency less than the resonance frequency. For the simulation purposes $f = 35000[Hz]$ is used and

the results of the calculation of the piezoelectric constants and also the equivalent circuit elements are shown in table 3.

Table 3: Values of piezoelectric constants in the second scenario

Material Constant	Value	Unit
Di-electric Constant	$d_{31} = 1.8857 \times 10^{-11} - 7.1079 \times 10^{-13} j$	$[C.N^{-1}]$
Electrical Permitivity at Constant Stress	$\epsilon_{33}^{T} = 1.6217 \times 10^{-8} - 3.6217 \times 10^{-10} j$	$[F.m^{-1}]$
C	$1.3496 \times 10^{-10} - 9.3424 \times 10^{-12} j$	$[F]$
C_0	$5.7706 \times 10^{-9} - 1.2255 \times 10^{-10} j$	$[F]$
L	$0.1255 + 0.0079 j$	$[L]$

The result of the simulation of the equivalent circuit is compared with the measurements and ElGhouti's result are shown in Fig. 13.

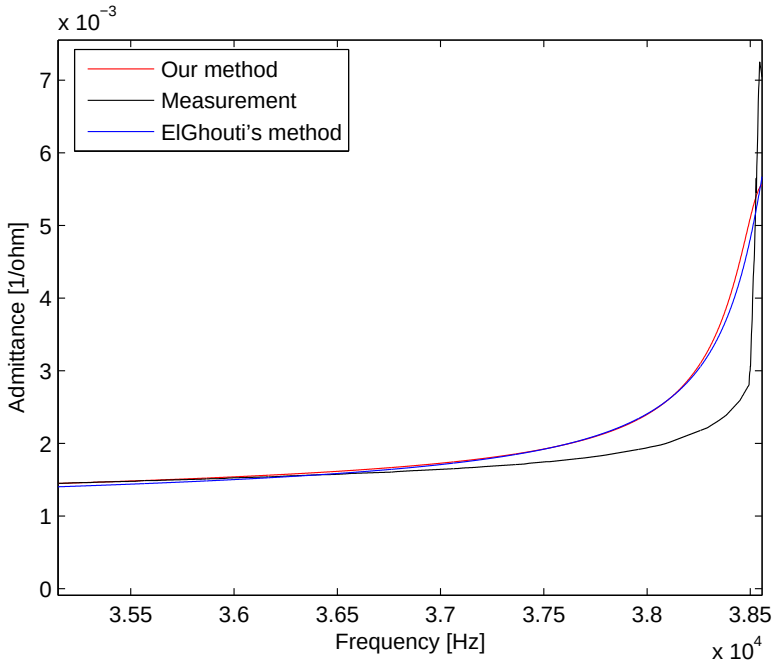

Figure 13: Comparison of the measurement of the admittance with the results of simulation for frequencies less than resonance frequency, f_s.

4 Discussion

By utilizing the results of the simulation, it is concluded that the suggested method based on using complex resonance frequency is modeling the admittance of the unloaded stator without using a large number of measurements for computing the constants of the material. Also it is presented that the new complex method is as

accurate as the method based on modeling with real numbers [4] for the frequencies below the resonance frequency whereas it models the admittance more accurately at the frequencies higher than the resonance frequency. It should be noted that the performance and efficiency of the motor at later frequency range is higher [24]. This means that our models suits modeling of the motor for later practical usages and control purposes.

Also it is suggested that care should be taken in solving Eq. (34) to find ϵ_{33}^{T} because the measurement error around the critical frequencies is higher than the frequencies which are above or below them therefore a small change in the frequency has a significant influence on the value of admittance.

5 Conclusion

In this report, we have investigated free stator modeling of rotary piezoelectric motor and proposed a complex numerical approach for modeling purposes. Also, the proposed method has been used for free stator modeling of Shinsei piezoelectric motor (USR60). It has shown that the model extracted by our method is more accurate than the model presented in [4] based on using real numbers for modeling. Further, the simulation shows that the new method is able to model the admittance of the motor at the interested frequecies which are higher than the resonance frequency.

References

[1] C. E. Land, G. W. Smith, , and C. R. Westgate, "The dependence of the small-signal parameters of ferroelectric ceramic resonators upon state of polarization," *IEEE Transactions on Sonics and Ultrasonics*, no. 1, pp. 8–19, 1964.

[2] T. Sashida and T. Kenjo, *An Introduction to Ultrasonic Motors*. Oxford Science Publications, 1993.

[3] B. Nogarede and E. Piecourt, "Modelisation of a traveling wave piezoelectric motor by equivalent electromechanical circuit," in *Proceeding of International Conference on ElecN. trical Machines (ICEM 94)*, vol. 2, 1994, pp. 128–133.

[4] N. ElGhouti, "Hybrid modeling of a traveling wave piezoelectric motor," Ph.D. dissertation, Department of Control Engineering, Aalborg University, 2000.

[5] T. Ikeda, *Fundamentals of Piezoelectricity*. Oxford University Press, 1996.

[6] D. Berlincourt, D. Curran, and H. Jaffe, "Piezoelectric and piezomagnetic materials and their function in transducers," in *Physical Acoustics-Principles and Methods*, 1st ed., W. Mason, Ed., 1967, vol. 1, no. A, ch. 3, pp. 169–270.

[7] B. Auld, *Acoustic Fields and Waves in Solids - Volume I*, 2nd ed. Krieger, 1990.

[8] R. Holland, "Representation of the dielectric, elastic and piezoelectric losses by complex coefficients," *IEEE Transaction on Sonics and Ultrasonics*, vol. 14, pp. 18–20, 1967.

[9] S. Sherrit, H. Wiederick, and B. Mukherjee, "Accurate evaluation of the real and imaginary constants for a piezoelectric resonator in the radial mode," *Ferroelectrics*, vol. 119, pp. 17–32, 1991.

[10] ——, "Non-iterative evaluation of the real and imaginary material constants of piezoelectric resonators," *Ferroelectrics*, vol. 134, pp. 111–119, 1992.

[11] A. V. Hippel, *Handbook of Physics*, 2nd ed. New York: McGraw-Hill, 1967.

[12] IEEE-Standard, "Ieee standard on piezoelectricity," IEEE/ANSI, 1987.

[13] J. Smits, "Iterative method for accurate determination of the real and imaginary parts of the material coefficients of piezoelectic ceramics," *IEEE Transaction on Sonics and Ultrasonics*, vol. 23, pp. 393–402, 1976.

[14] C. Alemany, L. Pardo, B. Jimenez, F. Carmona, J. Mendiola, and A. Gonzales, "Automative iterative evaluation of complex material constants in piezoelectric ceramics," *Journal of Physics D: Applied Physics*, vol. 27, pp. 148–155, 1994.

[15] C. Alemany, A. Gonzale, L. Pardo, B. Jimenez, F. Carmona, and J. Mendiola, "Automatic determination of complex constants of piezoelectric lossy materials in radial mode," *Journal of Physics D: Applied Physics*, vol. 28, pp. 945–956, 1995.

[16] M. Maeda, H. Hashimoto, and I. Suzuki, "Measurements of complex materials constants of piezoelectrics: extensional vibrational mode of a rectangular bar," in *Jurnal of Physics D: Applied Physics*, vol. 36, July 2003, pp. 176–180.

[17] K. W. Kwok, H. L. W. Chan, and C. L. Choy, "Evaluation of the material parameters of piezoelectric materials by various methods," *IEEE Transaction on Ultrasonics, Ferroelectrics, and Frequency Control*, vol. 44, no. 4, pp. 733–742, 1997.

[18] L. Armande, C. Miclea, and C. Tanasoiu, "Iterative evaluation of the complex constants of piezoceramic resonators in the radial mode," *Journal of the European Ceramic Society*, vol. 22, pp. 1873–1881, 2002.

[19] ——, "Iterative evaluation of the complex constants of piezoceramic resonators in the thickness mode," *Journal of the European Ceramic Society*, vol. 23, pp. 1145–1881, 2002.

[20] X. H. Du, Q. M. Wang, and K. Uchino, "An accurate method for the determination of complex coefficients of single crystal piezoelectric resonators i: Theory," *IEEE Transaction on Ultrasonics, Ferroelectrics, and Frequency Control*, vol. 51, no. 2, pp. 227–237, 2004.

[21] ——, "An accurate method for the determination of complex coefficients of single crystal piezoelectric resonators ii: Design of measurements and experiments," *IEEE Transaction on Ultrasonics, Ferroelectrics, and Frequency Control*, vol. 51, no. 2, pp. 238–248, 2004.

[22] ——, "Accurate determination of complex materials coefficients of piezoelectric resonators," *IEEE Transaction on Ultrasonics, Ferroelectrics, and Frequency Control*, vol. 50, no. 3, pp. 312–320, 2003.

[23] R. Holland and E. EerNisse, "Accuarte measurement of coefficients in a ferroelectric ceramic," *IEEE Transaction on Sonics and Ultrasonics*, vol. 16, no. 4, pp. 73–181, 1970.

[24] T. Senjyu, S. Yokoda, and K. Uezato, "A study on high efficiency drive of ultrasonic motors," in *Journal of Power Components and Systems*, vol. 29. Taylor & Francis, 2001, pp. 179–189.